# Constraining the QCD Phase Diagram by Tricritical Lines at Imaginary Chemical Potential

Philippe de Forcrand[1,2,*] and Owe Philipsen[3,†]

[1]Institut für Theoretische Physik, ETH Zürich, CH-8093 Zürich, Switzerland
[2]Physics Department, TH Unit, CERN, CH-1211 Geneva 23, Switzerland
[3]Institut für Theoretische Physik, Johann-Wolfgang-Goethe-Universität, 60438 Frankfurt am Main, Germany

(Received 28 April 2010; published 4 October 2010)

We present unambiguous evidence, from lattice simulations of QCD with three degenerate quark species, for two tricritical points in the $(T, m)$ phase diagram at fixed imaginary chemical potential $\mu/T = i\pi/3 \bmod 2\pi/3$, one in the light and one in the heavy mass regime. These represent the boundaries of the chiral and deconfinement critical lines continued to imaginary $\mu$, respectively. It is demonstrated that the shape of the deconfinement critical line for real chemical potentials is dictated by tricritical scaling and implies the weakening of the deconfinement transition with real chemical potential. The generalization to nondegenerate and light quark masses is discussed.

DOI: 10.1103/PhysRevLett.105.152001 PACS numbers: 12.38.Gc, 05.70.Fh, 11.15.Ha

The QCD phase diagram is at present largely unknown. It describes which different forms of nuclear matter exist for different choices of temperature and baryon density and whether they are separated by phase transitions. Its knowledge is thus of great importance for current and future experimental programs in nuclear and heavy ion physics as well as astroparticle physics. Since QCD is strongly coupled on scales of a baryon mass and below, fully nonperturbative calculations are warranted. Unfortunately, Monte Carlo simulations of lattice QCD at nonvanishing baryon density are prohibited by the "sign" problem. To date, only indirect methods are available, introducing additional approximations which are justified for $\mu/T \lesssim 1$ only [1]. One of these consists of simulating QCD at imaginary chemical potential $\mu = i\mu_i$ with $\mu_i \in \mathbb{R}$, for which there is no sign problem, and analytically continuing the results to real $\mu$ [2,3]. While Monte Carlo results contain all information about imaginary $\mu$, analytic continuation via truncated polynomials fitted to the data introduces the approximation.

In this Letter, we propose instead to study the phase diagram of QCD at imaginary chemical potential in its own right. We shall demonstrate that there are intricate first-order, triple, critical, and tricritical structures, whose details depend on the number of dynamical quark flavors $N_f$ and their respective masses $m_f$. These structures are *bona fide* properties of QCD and for this reason alone merit a detailed investigation. Moreover, we show that tricritical lines found at imaginary chemical potential, with their associated scaling behavior, represent important constraints for the critical surfaces at real chemical potential. Finally, the phase diagram we investigate may serve as a benchmark for studies within effective models (such as Polyakov-Nambu-Jona-Lasinio, sigma models, quark hadron models, etc.), which can be easily extended to imaginary $\mu$.

Here we present a study of the $(T, m)$ phase structure of QCD at fixed imaginary chemical potentials, $\mu_i^c = (2n + 1)\pi T/3$, $n = 0, \pm 1, \pm 2, \ldots$, for $N_f = 3$ degenerate quark flavors. At those values of $\mu_i$, QCD undergoes a transition between adjacent $Z(3)$ sectors. This is due to the exact symmetries of the partition function

$$Z(\mu) = Z(-\mu), \qquad Z\left(\frac{\mu}{T}\right) = Z\left(\frac{\mu}{T} + i\frac{2\pi n}{3}\right) \quad (1)$$

for complex $\mu$ [4], which imply $Z(\mu_i^c + \mu_i) = Z(\mu_i^c - \mu_i)$. The $Z(3)$ sectors are distinguished by the Polyakov loop

$$L(\mathbf{x}) = \frac{1}{3}\,\mathrm{Tr}\prod_{\tau=1}^{N_\tau} U_0(\mathbf{x}, \tau) = |L|e^{-i\varphi}, \quad (2)$$

whose phase $\varphi$ cycles through $\langle\varphi\rangle = n(2\pi/3)$, $n = 0, 1, 2, \ldots$, as the different sectors are traversed.

Hence, for complex $\mu$ there is a global $Z(3)$ symmetry, even in the presence of finite mass quarks. Transitions in $\mu_i$ between neighboring sectors are of first order for high $T$ and analytic crossovers for low $T$ [2–4], as shown in Fig. 1

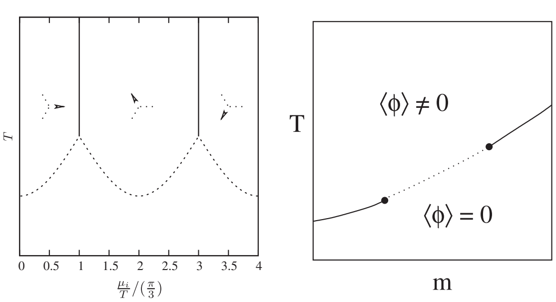


FIG. 1. Left: Phase diagram for imaginary $\mu$. Vertical lines are first-order transitions between $Z(3)$ sectors; arrows show the phase of the Polyakov loop. The $\mu = 0$ chiral or deconfinement transition continues to imaginary $\mu$; its order depends on $N_f$ and the quark masses. Right: Phase diagram for $N_f = 3$ at $\mu = i\pi T$. Solid lines are lines of triple points ending in tricritical points, connected by a line of $Z(2)$ critical points.

 

(left). Correspondingly, for fixed $\mu_i = \mu_i^c$, there are transitions in $T$ between an ordered phase with two-state coexistence at large $T$ and a disordered phase at low $T$. An order parameter to distinguish these phases is the shifted phase of the Polyakov loop, $\phi = \varphi - \mu_i/T$ [5]. At high temperature it fluctuates about $\langle\phi\rangle = \pm\pi/3$ on the respective sides of $\mu_i^c$. The thermodynamic limit picks one of those states, thus spontaneously breaking the reflection symmetry about $\mu_i^c$. At low temperatures $\phi$ fluctuates smoothly between those values, with the symmetric ground state $\langle\phi\rangle = 0$.

Away from $\mu_i = \mu_i^c$, there is a chiral or deconfinement transition line separating high and low temperature regions. This line represents the analytic continuation of the chiral or deconfinement transition at real $\mu$. Its nature depends on the number of quark flavors and masses. Early evidence [2,3] is consistent with this line meeting the $Z(3)$ transition at its end point between first order and crossover, and our present analysis unambiguously confirms this. The nature of the end point of the $Z(3)$ transition line has already been investigated for $N_f = 4$ [6] and more recently for $N_f = 2$ [7].

In this Letter, we study the nature of this junction at fixed $\mu = i\pi T$ in $N_f = 3$ QCD as a function of quark mass. There are two possibilities, which we shall find to be both realized. For small masses the chiral transition is first-order and branches off the $Z(3)$ transition line, rendering the meeting point of the three first-order lines a triple point. For intermediate masses, the $Z(3)$ transition ends in a second-order end point with 3D Ising universality; i.e., the chiral or deconfinement transition in its vicinity is a crossover. For large masses there is a first-order deconfinement transition meeting the $Z(3)$ transition again in a triple point. Hence, for fixed $\mu = i\pi T$, we obtain a $(T, m)$ phase diagram as in Fig. 1 (right). The end points of the solid lines, which separate triple points from Ising points, correspond to tricritical points. The change from first-order to Ising behavior for light and intermediate quark masses has already been observed for $N_f = 2$ [7].

To establish the phase diagram Fig. 1 (right) numerically, we work on lattices with temporal extent $N_t = 4$ with standard staggered fermions at fixed $\mu/T = i\pi$, using the rational hybrid Monte Carlo algorithm and setting aside possible issues with taking a fractional power of the fermion determinant. For fixed $N_t$, $T$ is tuned by varying the lattice gauge coupling $\beta$. For a given bare quark mass $am$, we investigate the nature of the transition as a function of $\beta$ by analyzing the finite-size scaling of the Binder cumulant

$$B_4(X) \equiv \langle(X - \langle X\rangle)^4\rangle / \langle(X - \langle X\rangle)^2\rangle^2, \tag{3}$$

with $X = \mathrm{Im}(L)$ and $\langle X\rangle = 0$. For $\mu/T = i\pi$, every $\beta$ value represents a point on the phase boundary and thus is pseudocritical. In the thermodynamic limit, $B_4(\beta) = 3$, 1.5, 1.604, and 2 for the crossover, first-order triple point, 3D Ising, and tricritical transitions, respectively. On finite $L^3$ volumes the steps between these values are smeared out to continuous functions whose gradients increase with volume. The critical coupling $\beta_c$ for the end point is obtained as the intersection of curves from different volumes. In the scaling region around $\beta_c$, $B_4$ is a function of $x = (\beta - \beta_c)L^{1/\nu}$ alone and can be expanded:

$$B_4(\beta, L) = B_4(\beta_c, \infty) + a_1 x + a_2 x^2 + \cdots, \tag{4}$$

up to corrections to scaling, with the critical exponent $\nu$ characterizing the approach to the thermodynamic limit. The relevant values for us are $\nu = 1/3$, 0.63, and 1/2 for a first-order, 3D Ising, or tricritical transition, respectively.

For each quark mass, we simulated lattices of sizes $L = 8$, 12, and 16 (20 in a few cases), at typically 8–14 different $\beta$ values, calculated $B_4(\mathrm{Im}(L))$ and filled in additional points by Ferrenberg-Swendsen reweighting [8]. Figure 2 shows examples for quark masses $am = 0.04, 0.3$. $B_4$ moves from large values (crossover) at small $\beta$ (i.e., low $T$) towards 1 (first-order transition) at large $\beta$ (i.e., high $T$). In the neighborhood of the intersection point, we then fit all curves simultaneously to Eq. (4), thus extracting $\beta_c$, $B_4(\beta_c, \infty)$, $\nu$, $a_1$, and $a_2$. We observe that the value of the Binder cumulant at the intersection can be far from the expected universal values in the thermodynamic limit. This is a common situation: Large finite-size corrections are observed in simpler spin models even when the transition is strongly first-order [9]. Moreover, in our case, logarithmic scaling corrections will occur near a tricritical point since $d = 3$ is the upper critical dimension in this case [10]. Fortunately, the critical exponent $\nu$, which determines the approach to the thermodynamic limit, is less sensitive to finite-size corrections and in Fig. 2 consistent with $\nu = 0.33$ and 0.63, its values for first- and second-order transitions, respectively. A check is to fix $\nu$ to one of the universal values and see whether the curves collapse under the appropriate rescaling, as in Fig. 2, insets. Note that the critical coupling determined from the intersection of the $B_4$ curves in Fig. 2 is consistent with the one extracted from the peak of the specific heat or the chiral susceptibility.

Proceeding in this way, we have investigated quark masses distributed over a large range, with results

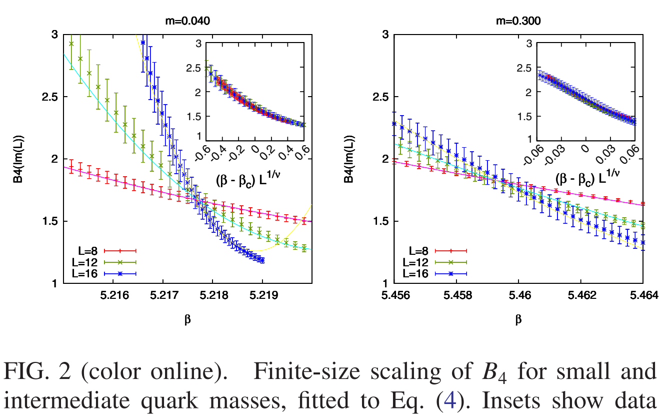


FIG. 2 (color online). Finite-size scaling of $B_4$ for small and intermediate quark masses, fitted to Eq. (4). Insets show data rescaled with the exponent fixed to $\nu = 0.33$ and 0.63, corresponding to a first- or second-order transition, respectively.

summarized in Fig. 3 (left). We find unambiguous evidence for a change from first-order scaling to 3D Ising scaling and back to first-order scaling as the quark mass is made larger. Note that, in the infinite volume limit, the curve would be replaced by a nonanalytic step function, whereas the smoothed-out rise and fall in Fig. 3 (left) corresponds to finite volume corrections.

The results from the finite-size scaling of $B_4$ can be further sharpened by looking at the probability distribution of $\mathrm{Im}(L)$ at the critical couplings $\beta_c$, corresponding to the crossing points. This is shown in Fig. 3 (right) for masses $am = 0.05, 0.1, 0.2, 0.3$ for $L = 16$. The lightest mass displays a clear three-peak structure, indicating coexistence of three states at the coupling $\beta_c$, which therefore corresponds to a triple point. The same observation holds for heavy masses. For $am = 0.1, 0.2$ the central peak is disappearing, and for $am = 0.3$ we are left with the two peaks characteristic for the magnetic direction of 3D Ising universality. We have checked the expected volume scaling of all distributions.

Hence, for small and large masses, we have unambiguous evidence that the boundary point between a first-order $Z(3)$ transition and a crossover at $\mu = i\pi T$ corresponds to a triple point. This implies that two additional first-order lines branch off the $Z(3)$ transition line as in Fig. 1 (left), which are to be identified as the chiral (for light quarks) or deconfinement (for heavy quarks) transition at imaginary chemical potential. This is expected on theoretical grounds: For $m = 0$ or $+\infty$, these transitions are first-order for any chemical potential. The fact that the end point of the $Z(3)$ transition line changes its nature from a triple point at low and high masses to second-order for intermediate masses implies the existence of two tricritical points. Our current data on $N_t = 4$ put these between $0.07 < am_{\mathrm{tric1}} < 0.3$ and $0.5 < am_{\mathrm{tric2}} < 1.5$.

Since our $N_t = 4$ lattice is very coarse, $a \sim 0.3$ fm, an important question concerns cutoff effects. These strongly affect quark masses and, in particular, the tricritical quark masses where the changes from a triple point to a critical Ising point happen. However, universality implies that critical behavior is insensitive to the cutoff, as long as the global symmetries of the theory are not changed. Our calculation is therefore sufficient to establish the qualitative picture Fig. 1 (right) as the continuum phase diagram at $\mu = i(2n+1)\pi T/3$ for $N_f = 3$.

Let us now discuss how this critical structure is embedded in the parameter space with nondegenerate quark masses [Fig. 4 (right)]. The case $N_f = 3$ corresponds to the diagonal, with two tricritical points separating triple points from second-order points. For nondegenerate quark masses, the qualitative possibilities for the junctions in Fig. 1 (left) remain the same. The tricritical points will thus trace out lines, $m_s^{\mathrm{tric}}(m_{u,d})$. In the case of heavy quarks, the situation is qualitatively the same for any $N_f = 1, 2, 3$ [11,12]. In the light quark regime, there is an interplay between the $Z(3)$ and chiral symmetries, and the situation may be more complicated. The findings reported in Ref. [7] imply the existence of a finite tricritical light quark mass also for $N_f = 2$. It would then seem natural that the tricritical points for $N_f = 2, 3$ are continuously connected by varying the strange quark mass, though this needs to be confirmed by explicit calculations. We stress that all critical structure indicated in Fig. 4 (right) can be determined reliably with Monte Carlo techniques and continuum extrapolations are feasible with current resources. Knowledge of the continuum phase diagram should provide valuable benchmarks for the description of QCD phases by effective models.

In order to establish the connection between imaginary and real chemical potential, let us briefly recall the situation at $\mu = 0$ [Fig. 4 (left)]. The deconfinement transition in pure gauge theory is first-order. In the presence of dynamical quarks, it weakens with decreasing quark mass until it disappears along the deconfinement critical line with 3D Ising universality. The critical point for $N_f = 1$ was determined in Ref. [12] and, more recently, for $N_f = 1, 2, 3$ in Ref. [11]. Similarly, the chiral transition for $N_f = 2 + 1$ is first-order and weakens with increasing quark mass, until it disappears at a chiral critical line with 3D Ising universality [13,14]. When a chemical potential is switched on, these critical lines sweep out critical surfaces, which continue in the imaginary $\mu$ (or $-\mu^2$) direction and join the tricritical lines [Fig. 4 (right)] at $\mu = i\pi T/3$. We

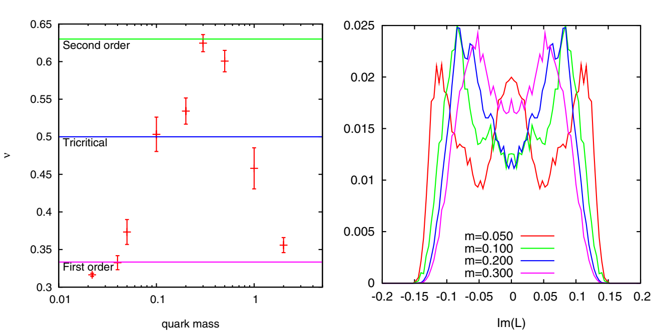


FIG. 3 (color online). Left: Critical exponent $\nu$ at $\mu/T = i\pi$. Right: Distribution of $\mathrm{Im}(L)$ at the end point of the $Z(3)$ transition.

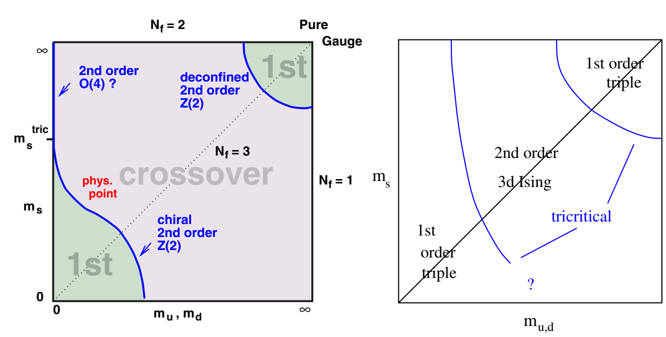


FIG. 4 (color online). Order of the transition as a function of quark masses. Left: The quark hadron transition at $\mu = 0$. Right: The $Z(3)$ transition end point at $\mu/T = i\pi/3$.

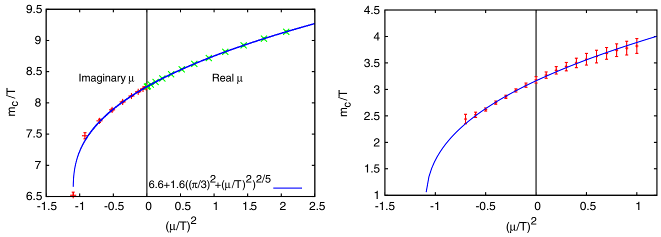


FIG. 5 (color online). Critical line $m_c(\mu^2)/T$ in the 3-state Potts model [15] (left) and for QCD in a strong coupling expansion [11] (right).

shall now illustrate this for the deconfinement critical surface.

By universality, the properties of a second-order transition are the same in a model sharing the same global symmetry, and for the deconfinement transition this is the 3D three-state Potts model with Hamiltonian

$$H = -k\sum_{i,\mathbf{x}}\delta_{\phi(\mathbf{x}),\phi(\mathbf{x}+\hat{\imath})} - \sum_{\mathbf{x}}[h\phi(\mathbf{x}) + h'\phi^*(\mathbf{x})], \quad (5)$$

where $\phi(\mathbf{x})$ is a $Z(3)$ spin and the couplings are identified as $h = \exp-(M-\mu)/T$ and $h' = \exp-(M+\mu)/T$, while $M$ is the heavy quark mass and $k$ increases with temperature $T$. The qualitative change of the critical deconfinement line with chemical potential can be calculated in this model, and one finds the first-order region to shrink with real $\mu$ [15]. The same observation is made for full QCD on a coarse lattice with a strong coupling expansion [11]. See Fig. 5.

Both calculations show the continuation of the critical mass to negative $\mu^2$ and a nonanalyticity when joining the $Z(3)$ transition at $\mu = i\pi T/3$. However, in both cases it has not been fully realized that this junction is tricritical. Since chemical potential enters the partition function of the Potts model in the same way as in QCD, it features the same $Z(3)$ transitions. We can therefore directly check our QCD results in the heavy mass region against those in the Potts model at the same value $\mu = i\pi T/3$. For the latter, the Binder cumulant of the spin magnetization was measured [15]. We reanalyzed those data, fitting them to the scaling form [Eq. (4)], and indeed find a change from first-order behavior ($\nu = 0.33$) at large values of $M/T$ to second-order 3D Ising ($\nu = 0.63$), implying again a tricritical point.

Generally, a tricritical point represents the confluence of two ordinary critical points. In the heavy mass region, the critical end points of the deconfinement transition at $\mu = i\pi T/3(1 \pm \varepsilon)$ merge with the end point of the $Z(3)$ transition. The deviation from the symmetry plane $[(\mu/T)^2 + (\pi/3)^2]$ corresponds to an external field in a spin model, and the way a critical line leaves a tricritical point in such a field is again universal [10]:

$$\frac{m_c}{T}(\mu^2) = \frac{m_{\rm tric}}{T} + K\left[\left(\frac{\pi}{3}\right)^2 + \left(\frac{\mu}{T}\right)^2\right]^{2/5}. \quad (6)$$

Figure 5 shows that the data from Refs. [11,15] excellently fit this form, far into the real chemical potential region. Thus, for heavy quark masses, the form of the critical surface of the deconfinement transition is determined by tricritical scaling of the $Z(3)$ transition at imaginary $\mu = i\pi T/3$.

It is clear that the chiral critical surface will likewise terminate on the chiral tricritical line at $\mu = i\pi T/3$. Unfortunately, for this surface no suitable effective model is available, and we presently do not know to what extent it is shaped by tricritical scaling. By estimating $am_{\rm tric1} \sim 0.1$ and using $am_c(0) \approx 0.0265$ [16], $K$ is fixed and expansion of Eq. (6) predicts a negative curvature $c_1 \approx -10$ for the chiral critical surface, as compared to the directly calculated $c_1 = -3.3(3)$ (in the notation of Ref. [16]). Tricritical scaling thus predicts a weakening also of the chiral phase transition with real chemical potential, independently confirming the findings in Refs. [2,14,16]. Whether the stronger effect is due to an inaccurate estimate of $m_{\rm tric1}$, finite-size or renormalization effects in both masses, or a deviation from tricritical scaling at $\mu = 0$ due to the interplay with chiral symmetry could be answered by extensive simulations.

*forcrand@phys.ethz.ch
†philipsen@th.physik.uni-frankfurt.de

[1] O. Philipsen, Proc. Sci., LAT2005 (2006) 016; JHW2005 (2006) 012; P. de Forcrand, Proc. Sci., LAT2009 (2009) 010.
[2] P. de Forcrand and O. Philipsen, Nucl. Phys. **B642**, 290 (2002).
[3] M. D'Elia and M. P. Lombardo, Phys. Rev. D **67**, 014505 (2003).
[4] A. Roberge and N. Weiss, Nucl. Phys. **B275**, 734 (1986).
[5] H. Kouno, Y. Sakai, K. Kashiwa, and M. Yahiro, J. Phys. G **36**, 115010 (2009).
[6] M. D'Elia, F. Di Renzo, and M. P. Lombardo, Phys. Rev. D **76**, 114509 (2007).
[7] M. D'Elia and F. Sanfilippo, Phys. Rev. D **80**, 111501(R) (2009).
[8] A. M. Ferrenberg and R. H. Swendsen, Phys. Rev. Lett. **63**, 1195 (1989).
[9] A. Billoire, T. Neuhaus, and B. Berg, Nucl. Phys. **B396**, 779 (1993).
[10] I. D. Lawrie and S. Sarbach, in *Phase Transitions and Critical Phenomena*, edited by C. Domb and J. L. Lebowitz (Academic, New York, 1984), Vol. 9, p. 1.
[11] J. Langelage and O. Philipsen, J. High Energy Phys. 01 (2010) 089.
[12] C. Alexandrou *et al.*, Phys. Rev. D **60**, 034504 (1999).
[13] F. Karsch, E. Laermann, and C. Schmidt, Phys. Lett. B **520**, 41 (2001).
[14] P. de Forcrand and O. Philipsen, J. High Energy Phys. 01 (2007) 077.
[15] S. Kim, Ph. de Forcrand, S. Kratochvila, and T. Takaishi, Proc. Sci., LAT2005 (2006) 166.
[16] P. de Forcrand and O. Philipsen, J. High Energy Phys. 11 (2008) 012.